Available at
www.ElsevierComputerScience.com
POWERED BY SCIENCE DIRECT®
Signal Processing 86 (2006) 1648–1655
SIGNAL PROCESSING
www.elsevier.com/locate/sigpro

A new IIR adaptive notch filter

Mu-Huo Cheng[a,*], Jau-Long Tsai[a]

[a]*Department of Electrical and Control Engineering, National Chiao Tung University, 1001 Ta Hsueh Road, Hsinchu 300, Taiwan*

Received 11 June 2003; received in revised form 2 May 2004
Available online 18 October 2005

Abstract

A new IIR adaptive notch filter (ANF) with fast convergence rate, accurate estimation of notch frequencies, and modest realization complexity is presented in this paper. The problem of obtaining a notch filter from a given signal containing multiple sine waves in noise is first formulated as the conventional problem of system identification. Then the new ANF is developed via the algorithm of Steiglitz McBride. Extensive simulations have been performed to verify the effectiveness of the ANF.

Keywords: Adaptive notch filter; System identification; Steiglitz Mc Bride method

1. Introduction

Adaptive notch filters (ANFs) are useful for detection, estimation, filtering, and tracking of sinusoidal signals in wideband noise environment. The ANF self-tunes its model parameters such that its notch frequencies can track the signal frequencies. Early ANFs [1] are realized by the finite impulse response (FIR) model. Recently, most ANFs use the infinite impulse response (IIR) model because it commonly requires a smaller number of parameters than the FIR one to characterize the sinusoidal signals.

Several IIR models have been used to develop the ANFs. The general IIR model was first proposed in [2]. Later, a more efficient IIR model which constrains model poles and zeros identical was used to derive ANFs [3–5]. Recently, Nehorai [6] and Ng [7], independently, developed ANFs using the most efficient IIR model for which the poles and zeros are not only identical but also located on the unit circle. Nehorai derived the ANF via the recursive maximum likelihood (RML) algorithm [6,8], while Ng developed the ANFs using the stochastic Gauss–Newton (SGN) as well as the approximate maximum likelihood (AML) algorithms [7].

Most recent ANFs, in our opinions, mainly focus on developing a better filter model. In this paper, we focus on developing a better ANF algorithm. We first formulate the problem of obtaining a notch filter as the conventional problem of system identification. Hence, many existing identification techniques can be applied for developing ANFs. From this perspective, the existing RML, SGL, and AML ANFs can be regarded to be developed via algorithms of the output-error formulation for system identification [9]. Since the Steiglitz–McBride method (SMM) [10] is well known for its

*Corresponding author. Tel.: +886 3573 1633; fax: +886 3571 5998.
E-mail address: mhcheng@cc.nctu.edu.tw (M.-H. Cheng).

0165-1684/$ - see front matter © 2005 Elsevier B.V. All rights reserved.
doi:10.1016/j.sigpro.2005.09.010

simple realization complexity, fast convergence rate, and proven convergence to the unbiased solution for off-line estimation and on-line adaptive IIR filters [11–13], we present a new ANF via SMM and explore its performance in this paper.

This paper is structured as follows: In Section 2, we derive the formulation and algorithm of the new ANF. Section 3 presents simulation results and the convergence properties of the ANF. Then, conclusions are made in Section 4.

2. SMM for adaptive notch filters

In this section, we first show that for a given signal containing multiple sine waves in noise finding a notch filter is equivalent to identifying a system. Then, the SMM algorithm for both identifying a system and finding a notch filter is discussed. Finally, the new ANF via SMM is developed.

2.1. System identification for notch filter

Consider a given signal which consists of a known number of sine waves and a measurement noise $e(n)$, given by

$$y(n) = \sum_{i=1}^{m} c_i \sin(w_i n + \phi_i) + e(n), \tag{1}$$

where the amplitudes $\{c_i\}$, phases $\{\phi_i\}$, and frequencies $\{w_i\}$ are unknown constants. It has been shown in [14] that $y(n)$ can be characterized as the output of an autoregressive moving average system excited by the measurement noise $e(n)$, i.e.,

$$A(q^{-1})y(n) = A(q^{-1})e(n), \tag{2}$$

where q^{-1} denotes a unit-delay operator and $A(q^{-1})$ is a monic polynomial of degree $2m$ with m coefficients $a_1, \ldots, a_m$, given by

$$A(q^{-1}) = \prod_{i=1}^{m} (1 - 2\cos w_i q^{-1} + q^{-2}) \tag{3}$$

$$= 1 + a_1 q^{-1} + \cdots + a_m q^{-m} + \cdots + a_1 q^{-(2m-1)} + q^{-2m}. \tag{4}$$

If $y(n)$ is used to excite a notch filter with the transfer function $A(q^{-1})/A(\rho q^{-1})$, $0<\rho<1$, as shown in Fig. 1, then we know from (2) that the filter output $\varepsilon(n)$ will approach $e(n)$ as the parameter ρ approximates 1. Hence, the problem to design a notch filter $A(q^{-1})/A(\rho q^{-1})$ is often formulated via Fig. 1 as an optimization problem to find filter coefficients $a_i, i = 1, \ldots, m$, for $\rho \to 1$ such that the mean square error of $\varepsilon(n)$ is minimized. That is,

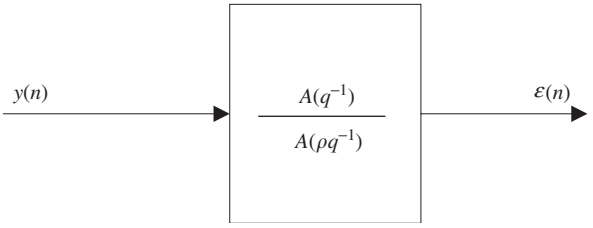

Fig. 1. A notch filter for a given signal $y(n)$.

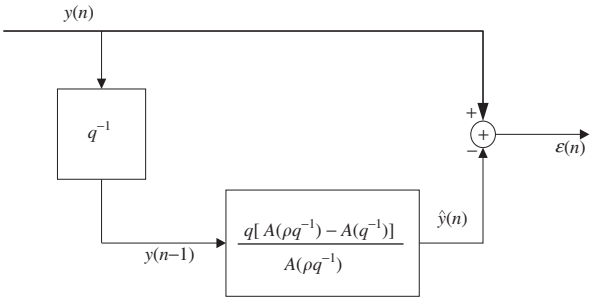

Fig. 2. The system identification configuration to obtain a notch filter from a given signal.

$$\min_{a_i, i=1,\ldots,m} E[\varepsilon^2(n)], \tag{5}$$

where $E[\cdot]$ denotes the expectation.

This problem can be expressed as a system identification problem by the simple manipulation

$$\frac{A(q^{-1})}{A(\rho q^{-1})} = 1 - \frac{A(\rho q^{-1}) - A(q^{-1})}{A(\rho q^{-1})} \tag{6}$$

$$= 1 - \frac{q^{-1}B(q^{-1})}{A(\rho q^{-1})}, \tag{7}$$

where

$$B(q^{-1}) = q[A(\rho q^{-1}) - A(q^{-1})] \tag{8}$$

$$= a_1(\rho - 1) + a_2(\rho^2 - 1)q^{-1} + \cdots + (\rho^{2m} - 1)q^{-(2m-1)}. \tag{9}$$

Thus, the configuration shown in Fig. 1 is equivalent to the configuration shown in Fig. 2; the problem of obtaining a notch filter from the given signal $y(n)$, therefore, is equivalent to identifying the model $B(q^{-1})/A(\rho q^{-1})$ excited by the input $y(n-1)$ such that the error between the model output $\hat{y}(n)$ and the desired signal $y(n)$ is minimized in the mean square sense.

The identification problem has been studied for several decades [9]; many identification techniques such as the output-error formulation, the equation-error formulation, and the Steiglitz–McBride method, therefore, can be applied to develop ANFs. Thus, existing RML, SGN, and AML ANFs [6,8,7] are just variants of the algorithms derived via the output-error formulation. Although the equation-error formulation can in theory be used to design a new ANF, it is in fact rarely used because its convergence solution is normally biased due to the measurement noise. In the followings, we exploit the SMM to develop a new ANF and investigate its performance.

2.2. SMM for notch filter

SMM [10] was proposed in 1965 as an ad hoc approach for off-line system identification. Later, SMM was shown in [15] that its convergence solution is unbiased when the model has sufficient order and the measurement noise is white. Since SMM often converges fast, has a theoretically proven unbiased convergence solution, and is simple to realize, it has been used in many off-line and on-line applications [11–13].

The block diagram of SMM for parameter identification from a given input $u(n)$ and output $y(n)$ of a plant is shown in Fig. 3. The algorithm initially sets the denominator polynomial $D_0(q^{-1})$ to a random value or unity and the index k to 1. The main SMM iteration for the index k determines both $D_k(q^{-1})$ and $N_k(q^{-1})$ such that the mean square error of $e_s(n)$ is minimized. Note that $e_s(n)$ is obtained under the fixed all-pole prefilters $1/D_{k-1}(q^{-1})$. Then the index is updated ($k = k + 1$) and the iteration continues until the obtained $D_k(q^{-1})$ converges. Finally, the plant $H(q^{-1})$ is modeled by the obtained $N_k(q^{-1})/D_k(q^{-1})$.

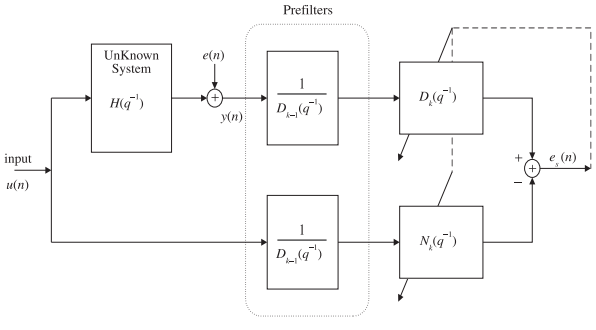

Fig. 3. The block diagram of SMM for system identification.

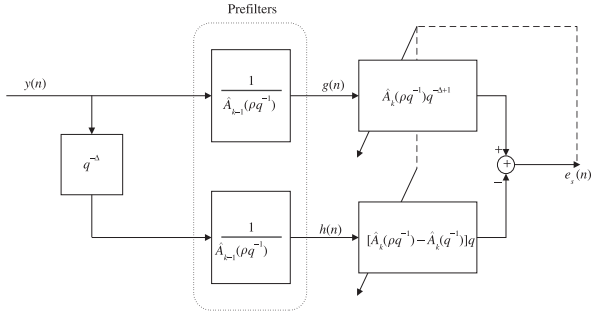

Fig. 4. The block diagram of SMM for notch filter identification.

Combining two block diagrams shown in Figs. 2 and 3 together, we can derive directly the block diagram, shown in Fig. 4, for finding a notch filter via SMM. Note that this block diagram is slightly modified because we introduce a delay parameter Δ instead of the unity constant. The main function of Δ is to remove the correlation between the noise component of $y(n)$ and that of $y(n-\Delta)$. Hence, the delay parameter is also called the decorrelation parameter [16]. This parameter, therefore, is introduced to cope with the effect arising from the colored noise $e(n)$. A judicious choice of the delay parameter may greatly reduce the bias caused by the colored noise contamination. Simulations, illustrated in the later section, will be used to verify its effectiveness.

2.3. The new adaptive notch filter

The new ANF via SMM can be derived directly from Fig. 4; its detailed algorithm is listed in Table 1. The algorithm is basically of the Newton-type adaptive filter. Some parameters in the algorithm and their functions are briefly discussed below.

The estimated coefficients at the nth iteration is expressed by $\hat{\boldsymbol{\theta}}(n)$, given by

$$\hat{\boldsymbol{\theta}}(n) = [\hat{a}_1(n), \ldots, \hat{a}_m(n)]^{\mathrm{T}}, \tag{10}$$

where the superscript T denotes the transpose. The number of frequencies in the signal is denoted by m. The delay parameter Δ, as discussed above, is used to cope with the colored measurement noise. The parameter λ, commonly referred to as the forgetting factor, is increasing at each iteration from the initial value (the nominal value is 0.7) to λ_∞ at the rate of the geometric ratio λ_r. Similarly, the parameter ρ is also increasing in the same way as λ from its initial value to ρ_∞ with the geometric ratio ρ_r. Note that

Table 1
The new ANF algorithm

Design variables: $m, \Delta, \lambda, \lambda_r, \lambda_\infty, \rho, \rho_r, \rho_\infty, \kappa$.

Initialization:

Nominal values: $\lambda = 0.7,\ \lambda_r = 0.99,\ \lambda_\infty = 0.995$

$\rho = 0.7,\ \rho_r = 0.99,\ \rho_\infty = 0.995$

$\kappa = 1$

$\hat{\boldsymbol{\theta}}(-1) = [0, \ldots, 0]^{\mathrm{T}}$

$P(-1) = \kappa I$

$h(i) = g(i) = 0$ for $i = -2m, \ldots, -1$

Main iteration loop: for $n = 0, \ldots, N$

$$g(n) = y(n) - \rho^{2m} g(n-2m) - \sum_{i=1}^{m-1} [\rho^i g(n-i) + \rho^{2m-i} g(n-2m+i)]\hat{a}_i(n-1) - \rho^m g(n-m)\hat{a}_m(n-1)$$

$$h(n) = y(n-\Delta) - \rho^{2m} h(n-2m) - \sum_{i=1}^{m-1} [\rho^i h(n-i) + \rho^{2m-i} h(n-2m+i)]\hat{a}_i(n-1) - \rho^m h(n-m)\hat{a}_m(n-1)$$

$$\psi_i(n) = \begin{cases} -\rho^i g(n-i-\Delta+1) - \rho^{2m-i} g(n-2m+i-\Delta+1) + (\rho^i - 1)h(n-i+1) + (\rho^{2m-i} - 1)h(n-2m+i+1), & i = 1, \ldots, m-1 \\ -\rho^m g(n-m-\Delta+1) + (\rho^m - 1)h(n-m+1), & i = m \end{cases}$$

$$\boldsymbol{\psi}(n) = [\psi_1(n), \psi_2(n), \ldots, \psi_m(n)]^{\mathrm{T}}$$

$$e_s(n) = g(n-\Delta+1) + \rho^{2m} g(n-2m-\Delta+1) - (\rho^{2m} - 1)h(n-2m+1) - \boldsymbol{\psi}^{\mathrm{T}}(n)\hat{\boldsymbol{\theta}}(n-1)$$

$$P(n) = \frac{1}{\lambda}\left[P(n-1) - \frac{P(n-1)\boldsymbol{\psi}(n)\boldsymbol{\psi}^{\mathrm{T}}(n)P(n-1)}{\lambda + \boldsymbol{\psi}^{\mathrm{T}}(n)P(n-1)\boldsymbol{\psi}(n)}\right]$$

$$\hat{\boldsymbol{\theta}}(n) = \hat{\boldsymbol{\theta}}(n-1) + P(n)\boldsymbol{\psi}(n)e_s(n)$$

$$\lambda = \lambda_r \lambda + (1 - \lambda_r)\lambda_\infty$$

$$\rho = \rho_r \rho + (1 - \rho_r)\rho_\infty$$

the parameter ρ determines the bandwidth of the notch filter; the closer to 1 is the parameter ρ, the narrower is the notch bandwidth. Smaller initial λ and ρ serve to increase the initial convergence speed of the ANF. The matrix P, called the correlation matrix inverse, is initially set to $P(-1) = \kappa I$ where I is an identity matrix and κ is a constant. The larger is the value κ, the faster is the convergence speed. Fast convergence speed, however, often results in a larger overshoot or undershoot of the estimated coefficients at each iteration.

3. Computer simulations and convergence properties

The ANF performance has been evaluated by extensive computer simulations. In this section, we present four simulations under various settings, demonstrating advantages and disadvantages of the new ANF. The first simulation demonstrates that the ANF can estimate multiple frequencies correctly. The second simulation shows the fast convergence speed and tracking capability of the ANF. The capability of the new ANF to estimate close frequencies in signal is illustrated in the third simulation. The last simulation illustrates the bias caused by the colored noise and the remedy by the properly chosen delay parameter. Then the ANF convergence properties are discussed.

3.1. Simulation 1

Let the signal be given by

$$y(n) = \sum_{k=1}^{4} c_k \sin(2\pi f_k n) + e(n), \tag{11}$$

where $f_1 = 0.1, f_2 = 0.2, f_3 = 0.3, f_4 = 0.4$, and $e(n)$ is a zero-mean and unit-variance white noise. The magnitude c_k of each sine wave is determined by the given signal-to-noise ratio (SNR). Here each sine wave is assumed to have identical SNR. Hence, if the SNR of each sine wave is 0 dB, then $c_k = \sqrt{2}$ for all k.

The ANF performance under various settings of the number of signal data N and SNR has been investigated. In each setting, 100 independent trials are performed. Simulation results are presented in Table 2 in which the bias, standard deviation, and Cramér–Rao bound (CRB) of each estimated frequency are shown. Note that the symbol with a number in parenthesis in Table 2 for $N = 100$ and SNR = 0 dB denotes the number of *outliers* in 100

Table 2
Simulation results of the new ANF: 100 independent trials for each case

N	SNR (dB)	Bias $\hat{f}_1$	St. dev. $\hat{f}_1$	Bias $\hat{f}_2$	St. dev. $\hat{f}_2$	Bias $\hat{f}_3$	St. dev. $\hat{f}_3$	Bias $\hat{f}_4$	St. dev. $\hat{f}_4$	CRB
		$\times 10^{-5}$	$\times 10^{-4}$	$\times 10^{-5}$	$\times 10^{-4}$	$\times 10^{-5}$	$\times 10^{-4}$	$\times 10^{-5}$	$\times 10^{-4}$	$\times 10^{-4}$
100	0	−9.09(2)	42.89(2)	−33.39(5)	38.63(5)	45.32(2)	42.80(2)	29.94(2)	42.36(2)	5.51
	4	−58.16	27.59	−22.41	31.66	8.25	23.62	55.95	32.80	3.48
	8	−31.60	19.11	−13.68	17.86	26.27	18.77	3.06	19.25	2.19
	12	−36.86	13.03	−1.34	10.19	−10.11	10.91	14.72	11.82	1.38
	16	−24.18	7.12	−1.56	7.52	−1.44	6.97	30.11	6.98	0.87
	20	−13.30	4.54	−3.80	4.44	1.64	4.60	21.71	5.22	0.55
		$\times 10^{-6}$	$\times 10^{-5}$	$\times 10^{-6}$	$\times 10^{-5}$	$\times 10^{-6}$	$\times 10^{-5}$	$\times 10^{-6}$	$\times 10^{-5}$	$\times 10^{-5}$
500	0	22.49	21.98	12.76	21.98	7.85	20.72	28.37	23.91	4.93
	4	5.72	14.75	−13.33	14.36	12.63	13.98	7.71	14.46	3.11
	8	−4.27	9.30	−4.75	9.33	−0.86	8.98	8.28	9.34	1.96
	12	−7.83	5.56	−7.58	5.51	−0.12	5.56	4.62	5.71	1.24
	16	−5.71	3.49	−6.78	3.71	0.57	3.65	6.05	3.53	0.78
	20	−10.04	2.45	−0.48	2.20	4.72	2.20	12.40	2.18	0.49
		$\times 10^{-7}$	$\times 10^{-6}$	$\times 10^{-7}$	$\times 10^{-6}$	$\times 10^{-7}$	$\times 10^{-6}$	$\times 10^{-7}$	$\times 10^{-6}$	$\times 10^{-6}$
2000	0	2.70	10.32	16.46	11.46	15.27	12.44	−2.67	10.49	6.16
	4	0.66	7.61	−6.25	6.66	3.57	6.92	3.54	6.80	3.89
	8	−0.53	4.12	6.95	4.17	−1.93	4.71	−10.84	4.68	2.45
	12	−0.89	2.54	−3.51	2.61	0.74	3.08	3.39	2.67	1.55
	16	0.82	1.62	1.50	1.96	−2.51	1.91	1.92	1.66	0.98
	20	−1.13	1.09	−0.79	1.16	−1.43	1.08	0.27	1.10	0.62

independent trials. The estimate is classified as an outlier if the absolute error between any one of the estimated and true signal frequency is more than 0.01.

This simulation shows that the ANF solution is unbiased. Moreover, its estimate is almost efficient because its standard deviation is close to the theoretic CRB. Compared with the results via RML–ANF shown in Table 3 in [6], we observe that under this setting, the presented ANF and RML–ANF both attain similar performance.

3.2. Simulation 2

The setting of this simulation is the same as Example 10.4 in [17]. The signal is given by

$$y(n) = \sqrt{2}\sin(2\pi f_1 n) + e(n), \tag{12}$$

where $e(n)$ is a white noise of unit variance. Note that the SNR in this example is 0 dB. The sinusoid frequency f_1 is switching abruptly every 1000 samples. For tracking, the ANF uses fixed λ and ρ. In this example, the ANF is simulated with $\lambda = 0.9$ and its estimated frequencies for $\rho = 0.7$ or $\rho = 0.9$ are shown in Fig. 5. Note that because a smaller ρ will widen the notch bandwidth, the convergence speed is faster but the estimate yields a larger ripple. Compared with the simulation results shown in [17], we observe that the new ANF exhibits fast convergence speed and excellent tracking capability.

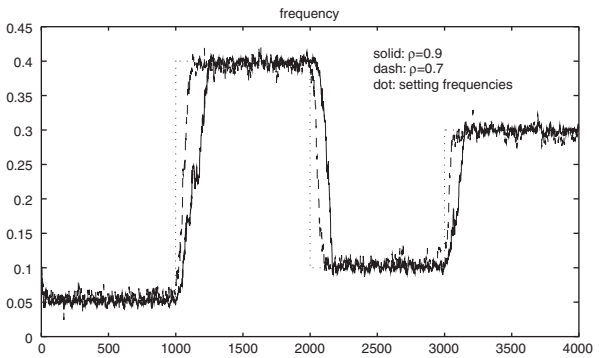

Fig. 5. The estimated frequencies versus time of the proposed ANF with $\lambda = 0.9$ and with $\rho = 0.7$ or $\rho = 0.9$.

3.3. Simulation 3

Although most existing ANFs suffer in estimating close signal frequencies, this simulation shows that the proposed ANF exhibits remarkable frequency discrimination capability. Let the signal comprise two sine waves and a measurement noise, given by

$$y(n) = c_1 \sin(2\pi f_1 n) + c_2 \sin(2\pi f_2 n) + e(n), \qquad (13)$$

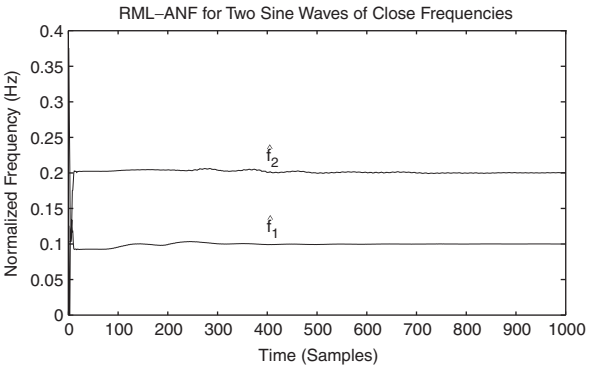

Fig. 6. The estimated frequencies versus time of the RML–ANF for SNR = 10 dB.

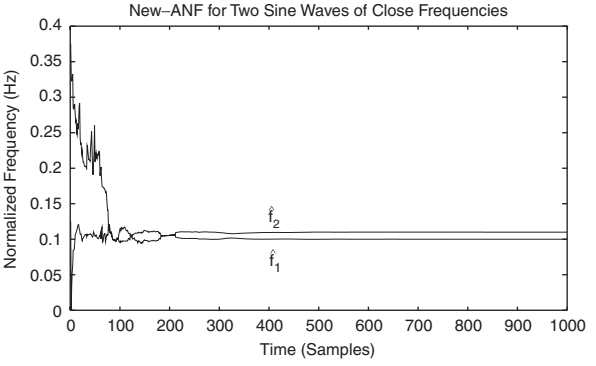

Fig. 7. The estimated frequencies versus time of the new ANF for SNR = 10 dB.

where $f_1 = 0.1$, $f_2 = 0.11$, and $e(n)$ is a zero-mean unit-variance white noise. Set SNR = 10 dB for each sine wave, we observe that RML, SGN, and AML ANFs all may fail to estimate signal frequencies correctly. For demonstration, the estimated frequencies via RML–ANF in one single trial are shown in Fig. 6 where the RML–ANF estimates only one frequency correctly. The new ANF, however, estimates both frequencies correctly, as shown in Fig. 7.

To further compare the frequency discrimination capability between the new ANF and RML–ANF, simulations for $f_1 = 0.1$ and several f_2 with SNR = 10 dB, $N = 1000$ have been performed and their results are listed, respectively, in Tables 3 and 4. Note that the proposed ANF always estimates frequencies correctly; the RML–ANF, however, often converges to an incorrect solution. When the frequency f_2 is closer to f_1, the RML–ANF more frequently obtains an incorrect estimate. As shown in Table 4, when $f_2 = 0.11$ the RML–ANF yields in an incorrect estimate 53 times out of 100 trials.

3.4. Simulation 4

One disadvantage of the proposed ANF is that it may end up with a biased solution when the noise is colored. This simulation demonstrates that a judicious choice of the delay parameter can lessen this effect. Let the signal for simulation be of the same form as (13), but the noise $e(n)$ be the output of a system with the transfer function $1/(1 - 0.8z^{-1})$ excited by a white noise with unit variance. The magnitudes c_1 and c_2 are determined by the assigned SNRs; note that the noise power here is 1/0.36.

The ANF estimate of a typical one trial for $f_1 = 0.1$, $f_2 = 0.2$ and SNR = 0 dB with $\Delta = 1$ or $\Delta = 30$ are shown in Figs. 8 and 9, respectively. For $\Delta = 1$, the colored noise makes the ANF solution biased, as shown in Fig. 8. For $\Delta = 30$, however,

Table 3
Simulation results of the new ANF: $f_1 = 0.1$, SNR = 10 dB, and several values of f_2

f_1	f_2	Bias $\hat{f}_1$	St. dev. $\hat{f}_1$	Bias $\hat{f}_2$	St. dev. $\hat{f}_2$
		$\times 10^{-6}$	$\times 10^{-5}$	$\times 10^{-6}$	$\times 10^{-5}$
0.1	0.20	−1.02	1.53	1.78	1.48
0.1	0.17	−2.55	1.41	0.90	1.56
0.1	0.15	−1.01	1.45	0.49	1.39
0.1	0.13	−4.50	1.39	3.27	1.59
0.1	0.11	−21.73	1.74	21.51	1.63

Table 4
Simulation results of the RML–ANF: $f_1 = 0.1$, SNR = 10 dB, and several values of f_2

f_1	f_2	Bias $\hat{f}_1$	St. dev. $\hat{f}_1$	Bias $\hat{f}_2$	St. dev. $\hat{f}_2$
		$\times 10^{-6}$	$\times 10^{-5}$	$\times 10^{-6}$	$\times 10^{-5}$
0.1	0.20	−2.12	2.21	−1.81	2.15
0.1	0.17	1.74(4)	2.16(4)	1.40(6)	1.79(6)
0.1	0.15	−3.21(21)	2.44(21)	5.39(22)	4.59(22)
0.1	0.13	−11.66(45)	5.79(45)	15.27(43)	16.66(43)
0.1	0.11	80.98(63)	14.56(63)	−94.31(53)	11.27(53)

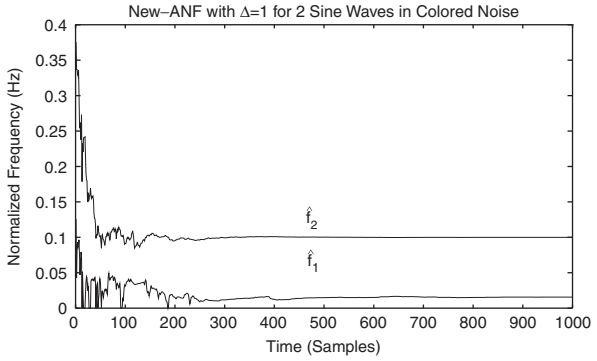

Fig. 8. The estimated frequencies versus time of the new ANF for $f_1 = 0.1$, $f_2 = 0.2$, SNR = 0 dB with $\Delta = 1$ in the colored noise environment.

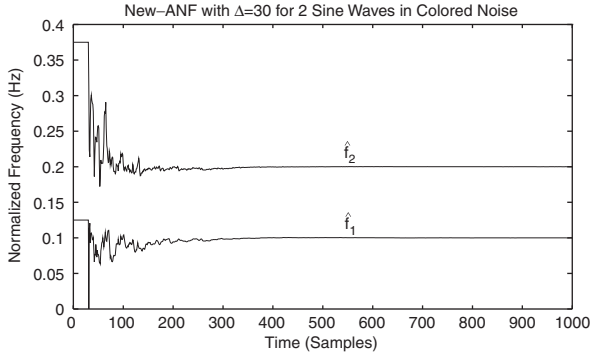

Fig. 9. The estimated frequencies versus time of the new ANF for $f_1 = 0.1$, $f_2 = 0.2$, SNR = 0 dB with $\Delta = 30$ in the colored noise environment.

because the colored noise of $y(n)$ and that of $y(n-\Delta)$ are almost uncorrelated, the ANF solution, shown in Fig. 9, is greatly improved. Therefore, a properly chosen delay parameter can greatly reduce the bias caused by the colored noise contamination.

3.5. Convergence properties

Extensive simulations indicate that the ANF always converges but its analytic proof is not available. The convergence solution of the proposed ANF, similar to the off-line SMM, can be shown to be unbiased when the model has sufficient order and the measured noise is white. This property is proven via the technique of ordinary differential equation (ODE) [18] in Appendix A. The proven unbiased solution also explains the powerful frequency discrimination capability of the new ANF.

4. Conclusions

This paper presents a new ANF via SMM. We first formulate the problem of determining a notch filter from a given signal as a system identification problem, then SMM is employed to develop the ANF. The new ANF exhibits fast convergence speed and an excellent capability to estimate close frequencies in signals. Simulations have been performed to verify the effectiveness of the proposed ANF.

Appendix A

In this appendix, we use the ODE technique [18] to show that the ANF convergence solution is unbiased when the model has sufficient order and the measurement noise is white.

The ODE approach, in essence, models the adaptive algorithm as a continuous time system which is described via the state-space representation by a set of ODEs. Hence, the ODEs can analyze the asymptotic behavior of the adaptive filter. Following the approach in [18] and denoting the correlation matrix and the coefficient vector of the ANF by $R(\tau)$ and $\hat{\boldsymbol{\theta}}(\tau)$, respectively, we obtain the ODEs for

the ANF, given by

$$\frac{\mathrm{d}\hat{\boldsymbol{\theta}}}{\mathrm{d}\tau} = R^{-1}\mathbf{f}(\hat{\boldsymbol{\theta}}), \tag{A.1}$$

$$\frac{\mathrm{d}R}{\mathrm{d}\tau} = G(\hat{\boldsymbol{\theta}}) - R, \tag{A.2}$$

where

$$\mathbf{f}(\hat{\boldsymbol{\theta}}) = \lim_{n\to\infty} E\{\boldsymbol{\psi}(n)[y(n) - \hat{\boldsymbol{\theta}}^{\mathrm{T}}\boldsymbol{\psi}(n)]\} = \mathbf{p}(\hat{\boldsymbol{\theta}}) - G(\hat{\boldsymbol{\theta}})\hat{\boldsymbol{\theta}}, \tag{A.3}$$

$$G(\hat{\boldsymbol{\theta}}) = \lim_{n\to\infty} E\{\boldsymbol{\psi}(n)\boldsymbol{\psi}^{\mathrm{T}}(n)\}, \tag{A.4}$$

$$\mathbf{p}(\hat{\boldsymbol{\theta}}) = \lim_{n\to\infty} E\{\boldsymbol{\psi}(n)y(n)\}, \tag{A.5}$$

and $\boldsymbol{\psi}(n)$ and $y(n)$ are defined in the algorithm.

Since (A.1) equals a zero vector in convergence and the matrix R is positive definite, the ANF convergence solution, denoted by $\hat{\boldsymbol{\theta}}^*$, can be obtained by solving the equation

$$\mathbf{f}(\hat{\boldsymbol{\theta}}^*) = \mathbf{p}(\hat{\boldsymbol{\theta}}^*) - G(\hat{\boldsymbol{\theta}}^*)\hat{\boldsymbol{\theta}}^* = \mathbf{0}. \tag{A.6}$$

Note that either the correlation matrix $G(\hat{\boldsymbol{\theta}}^*)$ or the cross-correlation vector $\mathbf{p}(\hat{\boldsymbol{\theta}}^*)$ can be decomposed into the sum of two terms, one for the sine wave signals and the other for the measurement noise because the signal and the noise are uncorrelated. Hence we can write

$$G(\hat{\boldsymbol{\theta}}^*) = G_{\mathrm{s}}(\hat{\boldsymbol{\theta}}^*) + G_e(\hat{\boldsymbol{\theta}}^*), \tag{A.7}$$

$$\mathbf{p}(\hat{\boldsymbol{\theta}}^*) = \mathbf{p}_{\mathrm{s}}(\hat{\boldsymbol{\theta}}^*) + \mathbf{p}_e(\hat{\boldsymbol{\theta}}^*), \tag{A.8}$$

where the subscripts s and e denote the effect of signal and noise, respectively. Substituting (A.7)–(A.8) into (A.6) and rearranging yields

$$\mathbf{p}_{\mathrm{s}}(\hat{\boldsymbol{\theta}}^*) + \mathbf{p}_e(\hat{\boldsymbol{\theta}}^*) = [G_{\mathrm{s}}(\hat{\boldsymbol{\theta}}^*) + G_e(\hat{\boldsymbol{\theta}}^*)]\hat{\boldsymbol{\theta}}^*. \tag{A.9}$$

Since the model is sufficient, if the signal contains no noise then the true system parameter, denoted by $\boldsymbol{\theta}_0$, will be the optimum solution for any $\hat{\boldsymbol{\theta}}^*$; that is,

$$\mathbf{p}_{\mathrm{s}}(\hat{\boldsymbol{\theta}}^*) = G_{\mathrm{s}}(\hat{\boldsymbol{\theta}}^*)\boldsymbol{\theta}_0. \tag{A.10}$$

Replacing this result into (A.9) yields

$$G_{\mathrm{s}}(\hat{\boldsymbol{\theta}}^*)(\boldsymbol{\theta}_0 - \hat{\boldsymbol{\theta}}^*) = G_e(\hat{\boldsymbol{\theta}}^*)\hat{\boldsymbol{\theta}}^* - \mathbf{p}_e(\hat{\boldsymbol{\theta}}^*). \tag{A.11}$$

Note that the terms in the right side of (A.11) represent the relation of the system shown in Fig. 4 with its input $y(n)$ containing the measurement noise only. Since the noise is white, we have

$$G_e(\boldsymbol{\theta})\boldsymbol{\theta} = \mathbf{p}_e(\boldsymbol{\theta}) \quad \text{for any } \boldsymbol{\theta}. \tag{A.12}$$

The above result and the property that the matrix G_{s} is positive definite enable us to conclude via (A.11) the unbiased convergence solution of the ANF, i.e., $\hat{\boldsymbol{\theta}}^* = \boldsymbol{\theta}_0$.

References

[1] B. Widrow, S.D. Stearns, Adaptive Signal Processing, Prentice-Hall, Englewood Cliffs, NJ, 1986.

[2] B. Friedlander, J.O. Smith, Analysis and performance evaluation of an adaptive notch filter, IEEE Trans. Inform. Theory 30 (2) (March 1984) 283–295.

[3] P.A. Thompson, A constrained recursive adaptive filter for enhancement of narrow-band signals in white noise, Proceedings of the 12th Asilomar Conference on Circuits, Systems and Computers, Pacific Grove, CA, November 1978, pp. 214–218.

[4] B.D. Rao, S.Y. Kung, Adaptive notch filtering for the retrieval sinusoids in noise, IEEE Trans. Acoust. Speech Signal Process. 32 (4) (August 1984) 791–802.

[5] B.D. Rao, R. Peng, Tracking characteristics of the constrained IIR adaptive notch filter, IEEE Trans. Acoust. Speech Signal Process. 36 (9) (September 1988) 1466–1479.

[6] A. Nehorai, A minimal parameter adaptive notch filter with constrained poles and zeros, IEEE Trans. Acoust. Speech Signal Process. 33 (4) (August 1985) 983–996.

[7] T.S. Ng, Some aspects of an adaptive digital notch filter with constrained poles and zeros, IEEE Trans. Acoust. Speech Signal Process. 35 (2) (February 1987) 158–161.

[8] P. Stoica, A. Nehorai, Performance analysis of an adaptive notch filter with constrained poles and zeros, IEEE Trans. Acoust. Speech Signal Process. 36 (6) (June 1988) 911–919.

[9] L. Ljung, T. Soderström, Theory and Practice of Recursive Identification, MIT Press, Cambridge, MA, 1983.

[10] K. Steiglitz, L.E. McBride, A technique for the identification of linear systems, IEEE Trans. Automat. Control 10 (1965) 461–464.

[11] H. Fan, W.K. Jenkins, A new adaptive IIR filter, IEEE Trans. Circuits Systems (October 1986) 939–947.

[12] P.M. Crespo, M.L. Honig, Pole-zero decision feedback equalization with a rapidly converging adaptive IIR algorithm, IEEE J. Sel. Areas on Communication (August 1991) 817–829.

[13] J.E. Cousseau, P.S.R. Diniz, New adaptive IIR filtering algorithms based on the Steiglitz–McBride method, IEEE Trans. Signal Process. 45 (5) (May 1997) 1367–1371.

[14] S.M. Kay, Modern Spectral Estimation, Prentice-Hall, Englewood Cliffs, NJ, 1988.

[15] P. Stoica, T. Söderström, The Steiglitz–McBride identification algorithm revisited—convergence analysis and accuracy aspects, IEEE Trans. Automat. Control 26 (6) (June 1981) 712–717.

[16] V.U. Reddy, B. Egardt, T. Kailath, Optimized lattice-form adaptive line enhancer for a sinusoidal signal in broad-band noise, IEEE Trans. Acoust. Speech Signal Process. 29 (3) (June 1981) 702–710.

[17] P.A. Regalia, Adaptive IIR Filtering in Signal Processing and Control, Marcel Dekker, New York, 1995.

[18] L. Ljung, Analysis of recursive stochastic algorithms, IEEE Trans. Automat. Control 22 (8) (August 1977) 551–575.